

15. Metal Nanoparticles

15.1. Surface plasmon resonances

In a bulk of conducting material (often, a metal), the free electrons can oscillate collectively with respect to the fixed ions. These oscillations occur at the plasma frequency ω_p and the associated quanta are called plasmons. In the Drude model, the electrons experience a friction force with damping time τ , giving rise to the following equation of motion for the polarization:

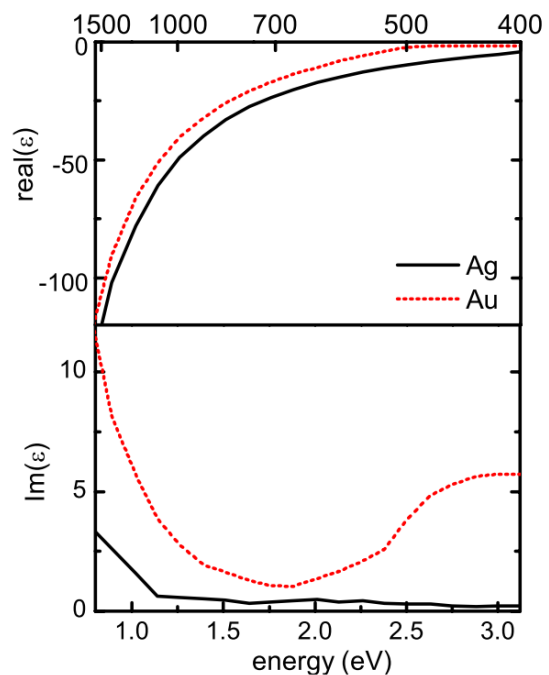
$$\ddot{\vec{P}} + \frac{1}{\tau} \dot{\vec{P}} = N \frac{e^2}{m} E$$

and the following dependence of the permittivity on frequency:

$$\varepsilon(\omega) = 1 - \frac{\omega_p^2}{\omega \left(\omega + \frac{i}{\tau} \right)}, \quad \text{with } \omega_p^2 = \frac{Ne^2}{m \varepsilon_0},$$

At the plasma frequency, and in the absence of damping, the dielectric permittivity $\varepsilon(\omega)$ goes to zero (the field is exactly compensated by the polarization, so that $\vec{D} = 0$). The plasma frequency is in the UV for many metals. Thus, in the near-infrared and visible, the polarization is nearly out of phase with the field, and the reflectivity of the metal is high.

Figure 15.1: Real and imaginary parts of the dielectric permittivity of noble metals, from Johnson and Christy (Phys. Rev. B 1972). Note the large values of the real part in the infrared and red for both metals, and the important value of the imaginary part in the green part of the visible for gold, responsible for its yellow color.



At a planar interface between a metal and a dielectric ϵ_1 , a surface plasmon polariton mode can propagate. At high wavevectors, corresponding to small wavelengths, the frequency of the surface plasmon is given by $\epsilon(\omega) = -\epsilon_1$. Small sizes correspond to the electrostatic limit. The field of the surface plasmon mode decays exponentially on both sides of the interface. The decay length in the metal is given by the optical skin depth:

$$\delta = \frac{c}{2\omega_p} \frac{1}{\sqrt{1 - \omega^2/\omega_p^2}} \approx \frac{c}{2\omega_p}$$

for low frequencies. In practice, this length is of the order of 20 nm.

In the case of a *small* spherical particle, in the electrostatic limit (radius of the particle much smaller than the wavelength, comparable to or smaller than the skin depth), the plasmon resonance frequency is obtained from the dependence of the dipole moment density \vec{P} of the sphere on the applied field \vec{E}_0 (Lorentz-Lorenz model):

$$\vec{P} = \frac{\epsilon(\omega) - \epsilon_1}{\epsilon(\omega) + 2\epsilon_1} \epsilon_0 \vec{E}_0 ,$$

which gives eigenmodes for $\epsilon(\omega) = -2\epsilon_1$.

These two examples (flat interface and sphere) show that the plasmon resonance depends on the dielectric in which the nanoparticles are contained, and depends also on the particle shape. For example, ellipsoids present three dipolar plasmon modes, with 3 different polarizations and up to 3 different frequencies. The width of the plasmon peak is related to the imaginary part of $\epsilon(\omega)$, which is particularly small for the noble metals Ag (throughout the near-infrared and visible) and Au (in the red and near-infrared; for Au at 800 nm, $\epsilon \approx -25 + 1.5 \times i$). These are the only metals discussed here. The dependence of their dielectric permittivity is shown in Fig. 15.1.

Because of the large electronic density and polarizability in metals, the field in the vicinity of metal structures can be very different from the applied field. A well-known example is the divergent electrostatic field in the vicinity of a sharp tip, known as the

lightning rod effect. In a similar way, the field is especially concentrated in the gap between two metal particles (see Fig. 15.2). The field is further enhanced by resonance if the frequency is resonant with that of a surface plasmon mode in the structure: this is the *resonance enhancement*. Depending on the size of the particles, on the gap, and on the wavelength, the field enhancement factor can reach or exceed 100. In larger and more complicated clusters of nanoparticles, even larger concentration factors of the field can arise in a few ‘hot spots’. This is demonstrated by calculations and by near-field optics experiments. The high field concentration is the basis for a wide range of optical experiments and applications involving metal structures at small scales, and known collectively as plasmonics. We shall see some examples in these lectures.

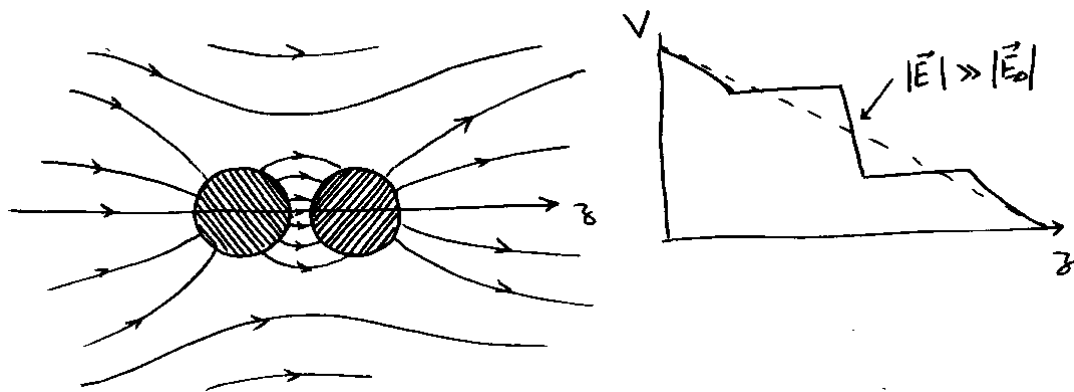


Figure 15.2 : Schematic illustration of the field concentration in the gap between a pair of metal spheres in the electrostatic approximation.

15.2. Synthesis of nanoparticles

15.2.1. Micro- and nano-lithography:

Modern lithography techniques reach resolutions of about 10 nm. It is therefore possible to fabricate gold or metal structures with this accuracy, using the standard techniques of semiconductor industry (writing in a photoresist, evaporation or sputtering of the metal, lift-off). The advantages of this fabrication method are the large freedom in shape and size of the objects. Disadvantages are the polycrystalline structure, the wetting layers often needed to ensure good adhesion of the noble metal on the substrate surface, and the lack of surface quality of the metal deposits.

15.2.2. Wet-chemical methods, seeded growth:

Wet chemical methods enable the production of many colloidal metallic particles. They start with the production of seeds, usually some nm in size, and include a controlled growth step ending up with a fairly monodisperse population of particles having more or less the same size and shape. The seeds can be single crystals, but can have more complex structures, such as the penta-twinned pyramids of gold. In a second step, larger nanoparticles are grown from the seeds in a growth solution. Growth solutions include surfactants to stabilize particles of a certain size and shape and catalysts favoring the growth of particular facets of the crystals. Illumination during growth can also drive the growth towards particular shapes such as triangular prisms for silver. Protocols have been discovered for the growth of balls, rods, cubes, bipyramids, octahedra, cages, dumbbells, stars or urchins, etc.

15.3. Optical detection methods

Different optical effects can be used for the detection of individual metal nanoparticles. In this section, we discuss detection at the same frequency as the probing laser. In the next sections, we shall discuss schemes involving the generation of new frequencies, either by luminescence or by nonlinear optical effects.

15.3.1. Dark-field scattering

This very simple method, first demonstrated by Zsigmondy around 1900, amounts to observing the light scattered by a metal particle in a direction where no light is observed in the absence of the particle. Under ideal conditions, the method would give an infinite signal-to-noise ratio, but scattering from substrate irregularities and other dielectric scatterers gives rise to a scattering background in all directions. In practice, even in very clean samples, this method works well only for particles larger than about 40 nm (gold). For big enough particles, its advantage is that it is simple to implement and easily provides spectral information analysis under white-light illumination.

15.3.2. Bright-field scattering, extinction, iSCAT

Here, one detects the change in the intensity of a reference field r (usually transmitted or reflected) caused by the addition of the small field s scattered by the particle. This change writes:

$$\Delta I = |r + e^{i\phi}s|^2 - |r|^2 \approx 2 \operatorname{Re}(rs \cos \phi)$$

where ϕ is a phase angle difference between the reference and the scattered fields. In the case of a small absorbing particle illuminated at resonance by a Gaussian beam, this phase difference is π . It combines the $\pi/2$ phase shift of the polarization at resonance, and the $\pi/2$ Gouy phase shift between the center of the spherical wave and the plane wave at large distances. The interference of the scattered field with the transmitted field is always *destructive*, and describes the attenuation, or *extinction*, of the transmitted field according to the optical theorem. The measurement of the transmitted field therefore corresponds to an extinction measurement, such as done in a spectrophotometer for molecules, for which this signal is identified with absorption. For suspensions of metal particles, extinction is caused by scattering as well as by absorption. The interference signal measured in extinction scales as the scattered *field* instead of the scattered *intensity*, and is therefore more favorable for the detection of small particles. The signal-to-noise ratio in this measurement, for shot-noise-limited measurements, is:

$$S/N = \frac{2sr \cos \phi}{\sqrt{r^2}} = 2s \cos \phi.$$

This expression shows that, for shot-noise-limited measurements, the signal-to-noise ratio is *independent of the strength of the reference field*. In particular, it is the same for transmission (extinction) and for reflection measurements. This important property makes it possible, without loss of signal-to-noise ratio, to adapt the measurement to experimental requirements, in particular detector sensitivity and laser amplitude noise, by choosing a convenient reference field.

15.3.3. Pump-probe time-resolved spectroscopy

In pump-probe microscopy, one does not directly measure the bright-field scattering of a particle, but rather the change in this bright field scattering signal caused by a pump or heating laser beam. This signal amounts to a difference between the intensity

scattered by the heated particle (after or while it absorbs the pump light) and the intensity scattered by the cold particle.

Performing this experiment with laser pulses is often called pump-probe spectroscopy. By following the time-resolved response of a single nanoparticle after a short-pulse excitation, one can distinguish the following regimes:

- i) the plasmonic response (duration less than 10 fs),
- ii) the response from hot electrons, which lasts from about one to a few ps, depending on the excitation intensity,
- iii) the coherent acoustic vibration response due to mechanical ringing of the particle, and eventually
- iv) the slow cooling of the particle's lattice and of its close surroundings, corresponding to heat diffusion towards the cooler environment. The thermal response is much slower than the electronic one and depends on particle size and observation length scale. It is of the order of a nanosecond for the particle, of a microsecond for the focal volume of a few hundred nanometers in size. On this longer timescale, the effect of the absorbed heat on the refractive index in the environment can be detected as photothermal contrast as explained hereafter. The mechanical vibrations of a particle can be used as probes for its mechanical properties.

15.3.4. Photothermal detection

Metal particles in dielectric samples present a high refractive-index contrast with their surroundings, and therefore give rise to strong light scattering. Observed in dark-field detection, the scattered intensity is proportional to the square of the volume of the particle, thus to the 6th power of its diameter. The absorbed energy, on the other hand, decreases only like the volume, i.e. the 3rd power of the diameter. For small enough particles, absorption will thus be easier to detect than dark-field scattering. Another drawback of scattering is that it cannot be spectrally or spatially discriminated from scattering by irregularities of the medium under study (e.g. organelles in a cell). But absorption is very difficult to measure. The absorption cross-section of a 5-nm gold particle at 514 nm is about 5 nm², only 100 times larger than that of a single dye molecule at room temperature. The saturation intensity of a metal particle, however, is many orders of magnitude higher than that of a molecule, because the lifetime of the plasmon states is very short. The maximum (or saturation) *absorption* of a metal particle is therefore several orders of magnitude larger than that of a molecule.

The slight temperature increase due to light absorption can be measured optically. It has two distinct physical origins, i) the change of the particle's optical properties with temperature, and ii) the small change of refractive index of the medium(s) surrounding the particle. We will not distinguish these effects in the rest of our discussion. This photothermal effect can be measured in various ways. The hotter volume around the absorbing object acts as a small divergent lens, which modifies the focusing, and therefore the intensity, of a focused probe beam. An alternative method is to measure the difference in optical phase between two neighboring beams, as first demonstrated in 2002 [D. Boyer et al., *Science* **297** (2002) 1160] and later improved by Lounis and colleagues [S. Berciaud et al., *Phys. Rev. B* **73** (2006) 045424]. Their method was a variant of a classical microscopy method 'differential interference contrast' (due to Nomarski). A green Ar⁺-ion beam was heating the metal particles, while a red He-Ne beam was used as a probe to measure the slight temperature increase due to absorption. The green beam was modulated at a high frequency (MHz), and the red signal demodulated at the same frequency. Finally, all three beams were scanned across the sample (as in confocal microscopy), to obtain a photothermal image of the sample.

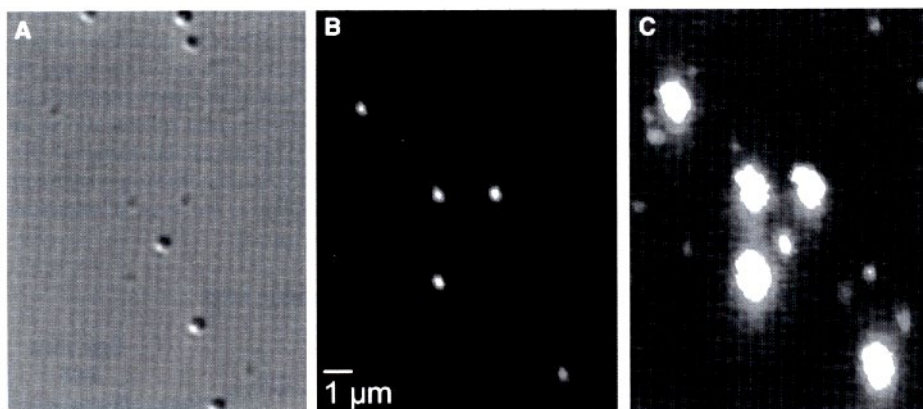


Figure 15.3 : Left : Differential interference contrast (DIC) image of latex beads, 80-nm and 10-nm Au beads. Only the latex beads and the 80-nm particles are seen. On the photothermal image at low heating power, only the 80 nm beads appear (center), while both kinds of particles appear on a photothermal image at high heating power (right).

Figure 15.3 shows an image of a glass surface, on which three kinds of particles have been deposited : 300-nm latex beads, 80-nm Au beads, and 10-nm Au beads. The latex beads appear clearly in the ordinary DIC image, but not in the photothermal images. The 80-nm beads can be seen in the DIC image, and much more clearly in the

photothermal image at low power. The photothermal image at the highest power shows the 10-nm beads, in addition to the strongly saturated 80-nm particles, but the 300 nm latex bead are completely absent.

The photothermal method enables following small Au labels (5 nm and below), which could be attached to biomolecules such as proteins. Their small size makes these labels very attractive to investigate the motion of proteins in crowded structures, such as synapses between nerve cells.

Photothermal detection has been applied to other individual nano-objects, in particular semiconductor nanocrystals, carbon nanotubes, conjugated polymer molecules and has been shown to enable the detection of single non-fluorescent dye molecules.